Research Article

Effect of Superabsorbent Polymer (SAP) Internal Curing Agent on Carbonation Resistance and Hydration Performance of Cement Concrete

Jieting Xu,[1] Xiao Qin [iD],[1] Zhenying Huang,[2] Yongkang Lin,[1] Ben Li,[1] and Zhengzhuan Xie[3]

[1]*Advanced and Sustainable Infrastructure Materials Group, School of Transportation and Civil Engineering and Architecture, Foshan University, Foshan 528225, Guangdong, China*
[2]*Guangzhou Huahui Traffic Technology Co, Ltd., Guangzhou 510355, China*
[3]*Guangxi Key Lab of Road Structure and Materials, Nanning 530007, Guangxi, China*

Correspondence should be addressed to Xiao Qin; qinnao@126.com

To clarify the influencing mechanism of superabsorbent polymer (SAP) internal curing agent on the carbonation resistance of cement concrete, accelerated carbonation experiment was conducted to explore the effect of particle size and dosage of SAP on carbonation depth. The hydration performance of internally cured concrete at different ages was studied by Fourier transform infrared spectroscopy (FTIR) test and X-ray diffraction (XRD) test. Combined with the scanning electron microscope (SEM) test, the hydration filling effect of internal curing on the microstructure of concrete was analyzed; meanwhile, the influence mechanism of SAP on carbonation resistance was revealed. The results showed that (i) when the particle size and dosage of SAP were 100 mesh and 0.200%, the carbonation depth of internally cured concrete was only 56.5% of the control group on day 28; (ii) the $Ca(OH)_2$ absorption peak area of SAP-concrete in the FTIR spectra could be increased by 3.38 times than that of the control group, and more C_2S and C_3S were translated into $Ca(OH)_2$, which helped to improve the hydration degree of cement concrete; (iii) the hydration products of day 56 were increased significantly and the remaining pores formed by SAP gels were gradually filled by hydration products, which enhanced the compactness and carbonation resistance of cement concrete.

1. Introduction

The corrosion of steel bars caused by carbonation is one of the main factors causing durability failure of concrete structures [1]. For bridge members, the carbonation reaction occurs accompanied by the erosion of acidic substances during the service period, which probably causes the destruction of passivation film, further the corrosion and expansion of steel bars [2]. Eventually, some cracks and spalling appear in the protective cover of concrete. In addition, microcracks caused by drying shrinkage and self-shrinkage are generated frequently due to the water evaporation and hydration reaction of concrete during the molding process, which probably provide several channels for CO_2 or other acidic substances to enter the concrete, accelerating the carbonation process. Therefore, the shrinkage microcrack must be suppressed to improve the carbonation resistance of concrete.

Internal curing is considered to be one of the most promising shrinkage and crack resistance technologies. The internal curing material incorporated in concrete can release some extra curing water in time to maintain high humidity internal environment and promote further hydration of the binding material. To date, SAP is one of the best internal curing materials with excellent water absorption and release properties [3–5]. Moreover, the effect of SAP on reducing the shrinkage and crack of concrete was proved, presented in relevant studies that the shrinkage decreased by approximately 31–41%, when the SAP dosage was 2.0% [6, 7].

For practical engineering, the investigation of carbonation resistance in concrete has application significance. Nevertheless, most of the existing research focuses on the

mechanical and engineering properties and durability, including frost resistance and antipermeability of internal curing cement concrete and mortar, but relatively few concentrate on carbonation resistance [8–11]. The specific studies status about this topic is shown as follows. The effect of SAP curing has been studied, and the experimental results of Beushausen et al. [12] and Shi et al. [13] showed that SAP could improve carbonation performance. Zhang et al. [14] found that the connectivity between pores was blocked by SAP after hygroscopic expansion by adding the appropriate amount of prewater absorption and preabsorption of 1% silver nitrate solution SAP in concrete, which would improve the carbonation resistance of concrete. Guo et al. [15] revealed the enhancing mechanism of SAP on carbonation resistance of concrete on the microscopic level.

The carbonation resistance of concrete mainly depends on the microcracks, which could be influenced by the hydration degree and products. As for the effect of SAP on hydration, Jiang et al. [16] found that the early hydration reaction (0-7d) of concrete was delayed by the addition of SAP. Zhao et al. [17] investigated the influence of nano-SiO$_2$ and SAP on the hydration process of early-age cement paste by the low-field nuclear magnetic resonance technology (LF-NMR). The result showed that the beginning time of each stage and the hydration duration were prolonged with the increase of SAP dosage. Qin et al. [18, 19] studied the microstructure of concrete through mercury intrusion porosimetry (MIP) and XRD, which concluded that the amount of ettringite was increased in concrete cured by SAP. Qin et al. [20] found that the hydration degree of concrete could be greatly improved by smaller-sized SAP in the long term by investigating the transformation rule of water form during the internal curing process.

The above research indicated that SAP had a positive impact on the carbonation and hydration performance of concrete. However, the existing research focuses on the direct index, including pores and microstructure, to study the influence of internal curing on carbonation resistance, and lacks the research on the interlock that how the hydration degree influences the compactness of the structure and reduces the microcracks, which affects the carbonation performance of concrete. Therefore, the relationship between hydration and carbonation also needs to be established to further explore the influencing mechanism on carbonation resistance. Otherwise, the engineering environment of the component was also important for its service performance, so it urgently needed to be considered. Nevertheless, former research has been conducted mainly in ordinary cement concrete, but few have been carried out for bridge deck concrete in hot and humid areas.

Regarding this situation, the factors including high CO$_2$ content, high temperature, and wet weather might accelerate the carbonation and the destruction of bridge deck concrete. In this case, the setting of each parameter in the carbonation test should be simulated to the actual engineering background. Meanwhile, it is necessary to illuminate the influencing mechanism of SAP on carbonation, which would promote its application in engineering to reduce durability damage caused by carbonation.

In this work, on the basis of fully considering the inherent properties of hot and humid regions, the varying rule of carbonation depth of cement concrete with SAPs of different particle sizes and dosages was studied by accelerated carbonation experiment. The hydration degree and products were investigated based on the FTIR and XRD tests. In addition, the Ca(OH)$_2$ absorption peak area of the control group and internal curing group at different ages was calculated quantitatively. In particular, an SEM test was conducted to observe the microstructure and remaining pores in concrete formed by SAP gels. Finally, the influencing mechanism of SAP on carbonation resistance was revealed by analyzing the carbonation depth, hydration performance, and microstructure characteristics of SAP-concrete.

2. Materials and Preparation

2.1. Materials

2.1.1. Superabsorbent Polymer (SAP).
Sodium polyacrylate SAP was used as an internal curing agent in this study, whose particle sizes included 221–864 μm (SAP-20), 117–140 μm (SAP-100), and 74–104 μm (SAP-150). SAP was a white particle or powder, and the microstructure of SAP dry powder is shown in Figure 1. The liquid absorption rate of SAP with different meshes in cement paste was tested using the tea bag method ($W/C = 0.37$). Table 1 presents the specific technical indices and the measured absorption rate of SAP.

2.1.2. Cement.
On the basis of GB 175–2020 [21], ordinary Portland cement (PO.42.5) with Blaine fineness of 3570 cm^2/g was selected in this article. The physical and mechanical properties are detailed in Table 2.

2.1.3. Aggregate.
The coarse aggregate (limestone) from Jiangmen, Guangdong Province in China, was used in this study, which included two types of 4.75–9.5 mm and 9.5–19 mm, and the applying mass ratio was 2 : 8. The fine aggregate was manufactured sand of fineness modulus of 2.80. The gradation curve is shown in Figure 2.

2.1.4. Water Reducer and Water.
Polycarboxylate superplasticizer (HPWR-Q8011) with a water reduction rate of 26% and a gas content of 2.5% was employed. Experimental water was Foshan tap water, which met the technical requirements of JGJ 63–2006 [22].

2.2. Mix Proportion of Concrete.
The theoretical internal curing water introduction amount and SAP content (mass ratio of binding materials) were calculated based on the SAP's water absorption in water at 30 min (see Table 1) and the Powers Formula (as (1)). In order to explore the effect of the dosage and particle size on carbonation resistance and hydration degree on cement, SAPs of three different particle sizes and dosages were applied in this study. The mix proportions of concrete used in this article are listed in Table 3. The mixing procedure is illustrated in Figure 3.
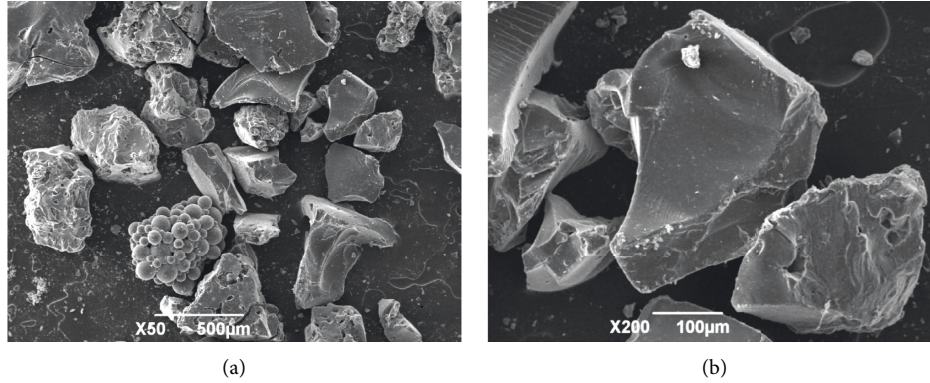
(a)

(b)

Figure 1: Micromorphology of SAPs in the dry state. (a) 50 times; (b) 200 times.

Table 1: Main technical indicators of SAP.

Density/(kg/ m^3)	pH/(1% moisture dispersion)	Saturated absorption time/s	Absorptance/(g/ g)	Water absorption/(g/g)		
				20–60 mesh	100–120 mesh	150–200 mesh
0.75	5.5–6.8	**< 28**	450–550	17.2	14.2	12.3

Table 2: Physical and mechanical properties of cement.

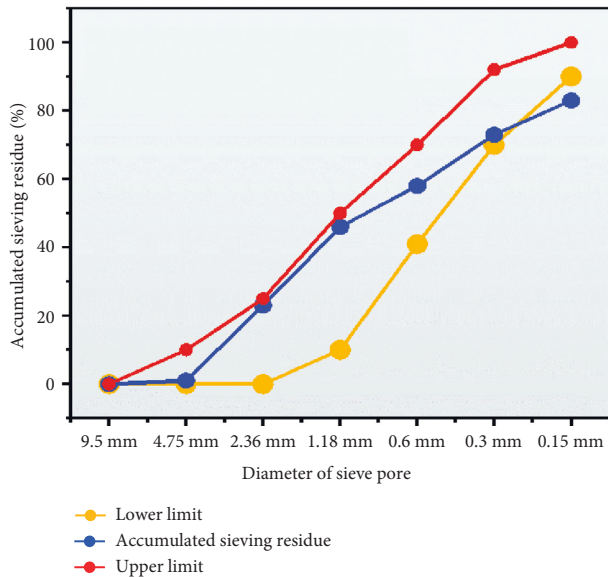| Normative indices	Setting time/min		Flexural strength/ MPa		Compressive strength/ MPa	
	Initial set	Final set	3 d	28 d	3 d	28 d
	203	450	5.9	7.7	27.4	45
PO.42.5	≥45	≤600	≥3.5	≥6.5	≥17.0	≥42.5

Figure 2: Fine aggregate gradation curve.

$$\frac{W}{C} \leq 0.36, \left(\frac{W}{C}\right)_{IC} = 0.18\left(\frac{W}{C}\right),$$
$$0.36 \leq \left(\frac{W}{C}\right)_{IC} \leq 0.42, \left(\frac{W}{C}\right)_{IC} = 0.42 - \left(\frac{W}{C}\right),$$

(1)

where $(W/C)_{IC}$ is the additional water-cement ratio required for internal curing.

3. Testing Method

3.1. Accelerated Carbonation Test. Carbonation resistance could be characterized by measuring the carbonation depth of concrete. The test (the process of the test, see Figure 4) was conducted by the HTX-12 concrete carbonation box produced by North-South Instrument and Equipment Co., Ltd. The carbonation resistance of concrete was tested after 28 days of curing according to JTG3420-2020 [23]. The test of carbonation depth was recorded on days 3, 7, 14, and 28. A similar specimen of 100 mm × 100 mm × 400 mm was prepared as a carrier for internal curing, which contained three parallel specimens in one group, and the bottom and surface were sealed with paraffin, leaving four sides. The specimens were placed in the testing space at 20 ± 5°C and 70 ± 5% RH and the concentration of CO_2 was 20 ± 3%. After testing treatment, the specimen was taken out and split on the press, and the thickness was decreased to 50 mm. The remaining specimen was put back in the carbonation box with a paraffin sealing section. The carbonation depth was calculated according to equation (2). Furthermore, in order to better investigate the influence of SAP on the carbonation performance of cement concrete, a coefficient of "relative carbonation rate" was defined and shown in equation (3).

TABLE 3: Mix proportion of internal curing pavement concrete.

| Concrete type | SAP | W_{IC}/(kg/m^3) | SAP dosage/kg | Compositions of pavement concrete/(kg/m^3) | | | | | |
				Cement	Water	Sand	4.75–9.5 mm Coarse	9.5–19 mm Coarse	Water reducer
S-Non	-	0	-						
S-20-0.200%	SAP-20	16.75	0.974						
S-150-0.200%	SAP-150	11.98	0.974	487	180.2	776	790	198	4.87
S-100-0.170%		11.76	0.828						
S-100-0.200%	SAP-100	13.83	0.974						
S-100-0.225%		15.56	1.096						

Step 1   Step 2   Step 3   Step 4
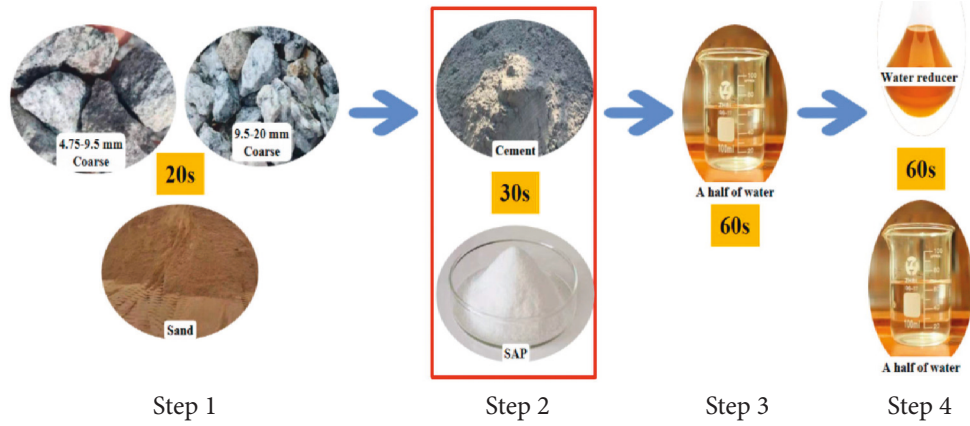
FIGURE 3: Preparing procedure of internal curing concrete with SAP.

Concrete carbonation test chamber   Wax sealing   Carbonizing   Splitting   Phenolphthalein spraying
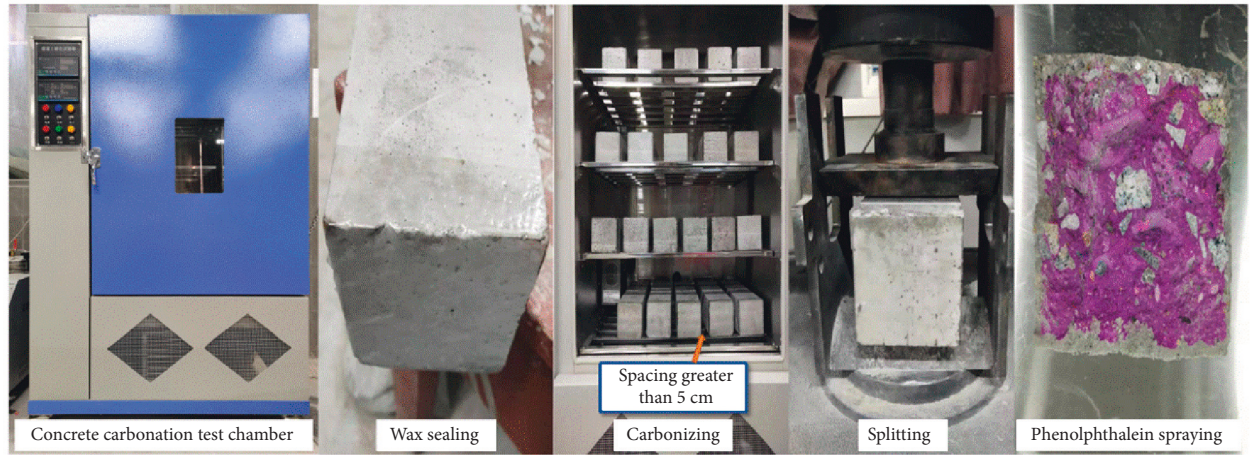
FIGURE 4: Process of concrete carbonation test.

$$\overline{d}_t = \frac{1}{n} \sum_{i=1}^{n} di, \qquad (2)$$

where $\overline{d}_t$ is the average carbonation depth (mm) after carbonation (d); d_i is the carbonation depth of each measuring point (mm); n is the total number of measuring points. (Each specimen included 10 data in this study.)

$$\alpha_R = \frac{d_n}{d_0}, \qquad (3)$$

where α_R is the relative carbonation rate; d_n is the average carbonation depth (mm) of the SAP curing group at different ages; d_0 is the average carbonation depth (mm) of the control group at different ages.

3.2. Hydration Performance Test

3.2.1. FTIR Test. To investigate the hydration degree of different experimental groups in Table 3, the FTIR test was carried out by FTIR-960 Fourier transform infrared spectrometer. The samples (approximately 0.02 g) were made with potassium bromide into thin slices using the specimen at the curing age of day 3, day 14, day 28, and day 56, respectively. The schematic of this test is presented in

Figure 5(a). The scanning wave number range was 4000–400 cm^{-1} and the resolution was 4.0 cm^{-1}.

It is worth noting that there were few studies on quantitative analysis of cement composition based on the FTIR technique [24]. A method for quantitative analysis of hydration degree was applied in this article. The absorption peak area of Ca(OH)$_2$ was quantitatively compared S-Non with the optimal SAP curing group. The tangent of the extreme points on both sides of the absorption peak was selected as the corrected baseline to calculate the absorption peak area, the baseline positioning, and peak area calculation (O$_1$, O$_2$, and O$_3$ are the reference points for peak area calculation), as shown in Figure 5(b).

3.2.2. XRD Test.
In order to further explore the influence of internal curing material on the internal hydration degree of cement, XRD was performed to characterize the valuation of hydration products. The samples chosen in this test contained three different curing ages of day 3, day 14, and day 28. The analysis angle range was 5°–80° with 40 kV voltage and 40 mA current.

3.3. SEM.
The carbonation resistance of internal curing concrete was closely related to its microstructure, and the macroscopic properties might be explained. Thus, SEM was used to characterize the microstructure and hydration products of concrete by a Japan Hitachi coldfield scanning electron microscope. The secondary electron resolution of SEM is 1.4 nm, and the magnification was 5000 times and 10000 times.

4. Results and Discussions

4.1. Influence Mechanism of Carbonation Resistance

4.1.1. Carbonation Resistance of Concrete with SAP of Different Particle Sizes.
The carbonation depth variation and relative carbonation rate of concrete with SAP of different particle sizes are shown in Figures 6 and 7, respectively.

From Figure 6, it can be seen that the incorporation of SAP had different effects on the carbonation resistance of concrete and the carbonation depth increased step by step with the extension of age. Among them, 100 mesh SAP had the minimum carbonation depth at the given time, followed by 150 mesh, which indicated that 100-mesh SAP had the best improvement effect on concrete. From the view of the relative carbonation rate in Figure 7, it can be discovered that the carbonation depth of the S-100-0.200% and S-150-0.200% groups were 56.5% and 88.3% compared to that of the control group on day 28, respectively. This phenomenon may be related to the distribution and internal curing range of SAP particles in concrete. The liquid absorption rate of 100 mesh is higher than 150 mesh, so the curing range of 100 mesh SAP internal curing water is larger, which reflects the better carbonation resistance.

Based on the above analysis, it can be speculated that for the given dosage, the larger the particle size is, the larger the curing range is provided, and the excellent carbonation

resistance may be presented. But it was interesting to find that the carbonation depth of the curing group was deeper than that of S-Non when the mesh was 20. Otherwise, the carbonation depth of concrete with 20-mesh SAP was 50.3% higher than that of the control group on day 3, but on day 28, only 9.9%, which demonstrated that the carbonation effect of 20-mesh SAP was gradually improved with the extension of age. In addition, SAP of 20 mesh may promote the generation of large remaining pores due to the large particle size of SAP and high liquid absorption rate, resulting in more channels for CO$_2$ to enter the internal concrete.

4.1.2. Carbonation Resistance of Concrete with SAP of Different Dosages.
To search the effect of SAP dosage on carbonation resistance, 3 dosages of 100-mesh SAP were chosen in this section, and the results are presented in Figures 8 and 9.

As shown in Figures 8 and 9, the carbonation resistance of concrete was enhanced to a certain degree. With the increase of SAP dosage, the carbonation depth of concrete decreased first and then increased on day 28. As the results show, the carbonation depth of internal curing groups of S-100-0.175%, S-100-0.200%, and S-100-0.225% were 9.0%, 24.7%, and 14.0%, respectively, less than that of the control group, while on day 28, there were 35.8%, 43.5%, and 18.2%, respectively, which decreased more significantly. Based on this phenomenon, it could be concluded that the dosage of 0.225% has the worst carbonation resistance among different dosages. Moreover, with the increase of age, the improving effect of internal curing material SAP on the carbonation resistance of cement concrete became more obvious. The addition of SAP could enhance the carbonation resistance of concrete, which could be interpreted as that SAP can absorb more internal curing water and gradually release the water absorbed in the mixing process during curing age, improving the relative humidity of concrete under the action of difference ion concentration and humidity. In this case, the microcracks in concrete are reduced, which could block the channels of CO$_2$ effectively. Therefore, the carbonation resistance of concrete is enhanced.

There is no doubt that the larger the curing range is, the more the microcracks may be inhibited, benefitting from the curing effect with the greater dosage, but it was interesting to note that the great dosage of 0.225% had the deepest carbonation depth. This is because the "microagglomeration" phenomenon is easy to occur in the process of cement concrete mixing, and the unsaturated SAP is wrapped with a layer of SAP saturated with water, which leads to further absorption of internal curing water being hindered and the internal curing effect weakened. In consequence, the carbonation resistance could be improved with a moderate dosage of SAP.

4.2. Hydration Degree Analysis Based on FTIR and XRD

4.2.1. Analysis of FTIR Spectra.
The influence of SAP on the hydration degree of cement could be inferred by the vibration peaks of each functional group measured by the FTIR test. The FTIR spectra of the control group
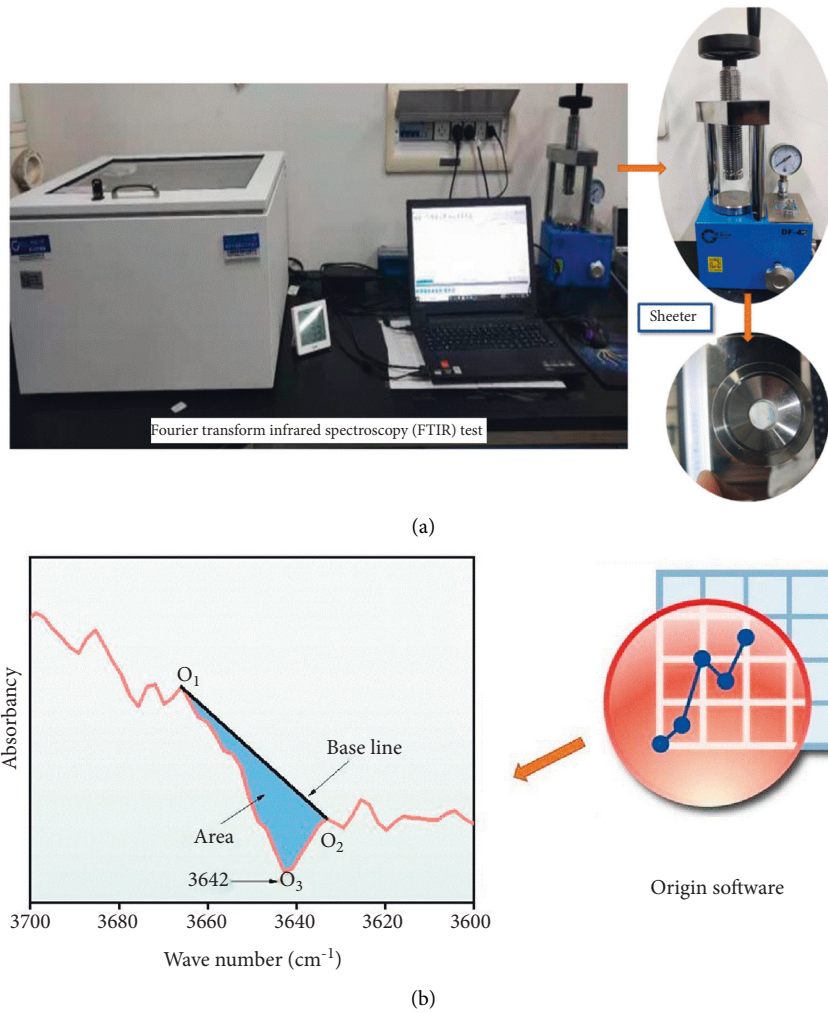
(a)

(b)

FIGURE 5: FTIR test: (a) process of preparation of thin slice samples; (b) calculation of peak area of $Ca(OH)_2$.
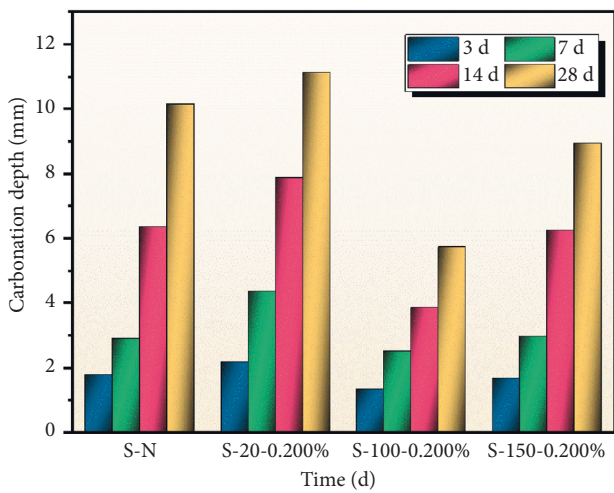

FIGURE 6: Carbonation depth of concrete with SAP of different sizes.
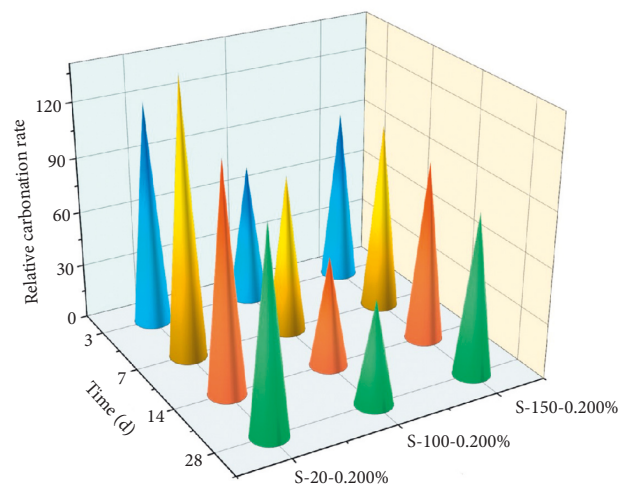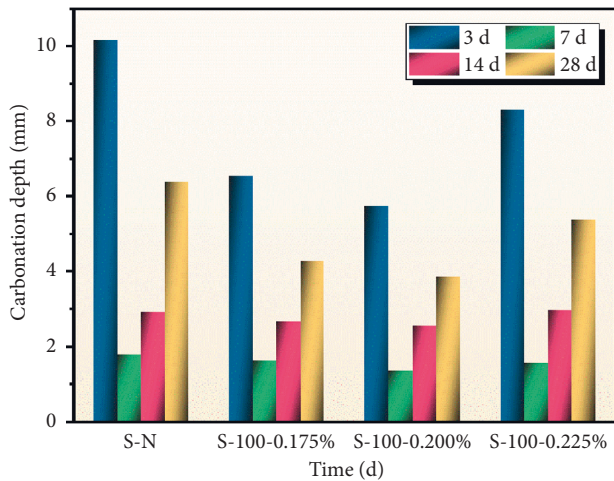

FIGURE 7: Relative carbonation rate of concrete with SAP of different sizes.

(Figure 10(a)) and S-100-0.200% (Figure 10(b)) (optimal group in carbonation test) were investigated and compared, whose age ranged from day 3 to day 56. At the same time, the effect of SAP particle size on the hydration of cement was studied by analyzing the FTIR spectra of day 56 (Figure 11).

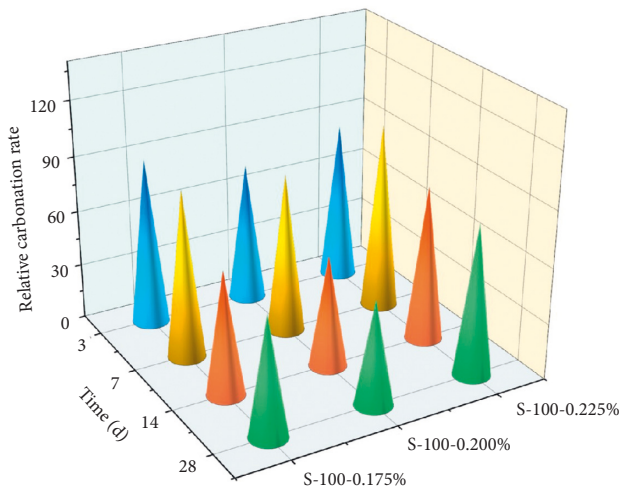Figure 8: Carbonation depth of concrete with SAP of different dosages.

Figure 9: Relative carbonation rate of concrete with different dosages.

From Figures 10 and 11, it can be observed that the position and shape of the characteristic peaks of each functional group were basically the same in FTIR spectra between the two groups, but the absorption intensity of the absorption peak was different, which indicated that the addition of SAP promoted the hydration process of cement and led to the relative content variation of cement concrete components. The functional groups of OH^- and CO_3^{2-} mainly appeared in the high wavenumber region from 4000^{-1} to $300 \, cm^{-1}$ and the stretching vibration peak of H-O-H (near $3432 \, cm^{-1}$) was the absorption peak of water molecules. The characteristic peak of $CaCO_3$ ($1423 \, cm^{-1}$) was caused by the CO_3^{2-} formed from the reaction of the alkali in the cement and CO_2 in the air, which induced the 'carbonation' phenomenon appearing in the cement. Therefore, the contact between CO_2 and H_2O should be avoided during the preparation, storage, and test of samples.

The absorption peak (below $1300 \, cm^{-1}$) was caused by the vibration of the silica or alumina groups and the asymmetric stretching vibration peaks of Si-O in the silica tetrahedron around $1081 \, cm^{-1}$ and $1024 \, cm^{-1}$. The bending vibration peak of Si-O-Si (around $692 \, cm^{-1}$) identified the degree of polymerization of the silicate grid, and the higher the peak value was, the higher degree of polymerization would be. The above peaks of Si-O and Si-O-Si combined with the bending vibration peak in the Si-O plane ($463 \, cm^{-1}$) corresponded to the characteristic peaks of the C-S-H gel. Vibration peaks of Al-O ($874 \, cm^{-1}$) were related to the generation of AFt or AFm. Although the variation of the main peak was not obvious with the advancement of the hydration process, the peak type of several small peaks in the range of $1300 \, cm^{-1}$–$450 \, cm^{-1}$ absorption peak developed rapidly. It could be explained that the aggregation degree of silicon (aluminum) oxygen polyhedron network structure on the surface of cement particles decreases, which leads to the tendency to be single in the oligomeric structure; thus, the symmetry of the structure is improved.

Figure 11 presents the FTIR spectra of concrete with SAP of different particle sizes at day 56. Compared with the S-Non, the characteristic peaks of hydration products of the internal curing group with 0.200% dosage were strengthened. The characteristic peak of the internal curing group was significantly enhanced to be about $874 \, cm^{-1}$, and the absorption peak area of $Ca(OH)_2$ in S-100-0.200% was the largest, which demonstrated the degree of hydration was high, followed by 150 mesh. Meanwhile, the water absorption was improved with the increase in particle size, which was attributed to the hydration of cement.

As for the effect of SAP dosage on the hydration degree of cement, it was quantitatively analyzed by calculating the area ratio of $Ca(OH)_2$ absorption peak of the internal curing group with SAP of various dosages and S-Non at different ages (Figure 12).

It can be seen in Figure 12 that the ratio of $Ca(OH)_2$ absorption peak ($3642 \, cm^{-1}$) shows the trend of decreasing-increasing in the SAP curing group and control group at different ages. The $Ca(OH)_2$ absorption peaks of S-100-0.175%, S-100-0.200%, and S-100-0.225% were 1.92 times, 1.95 times, and 1.74 times than that of the control group, respectively. It could be concluded that the early hydration of cement concrete can be enhanced with the addition of SAP. Interestingly, it was found that the absorption peak of $Ca(OH)_2$ in internal curing groups with three particle sizes was smaller than that S-Non at day 28. This phenomenon could be interpreted that the internal humidity of cement concrete gradually decreases with the continuous hydration. Then the internal water is gradually released, which promotes the secondary hydration of unhydrated cement and some part of $Ca(OH)_2$ is consumed. Thus, the hydration degree in the later stage is improved effectively. Compared with the control group at the age of day 56, SAP curing groups increased by 0.7 times, 3.36 times, and 1.03 times, respectively.

According to the above results, the dosage of 0.200% is considered the optimal dosage, which has the best enhancing effects. With the appropriate particle size and dosage, the hydration degree of cement can be improved and internal microcracks may be reduced, which would enhance structural compactness and promote carbonation resistance.
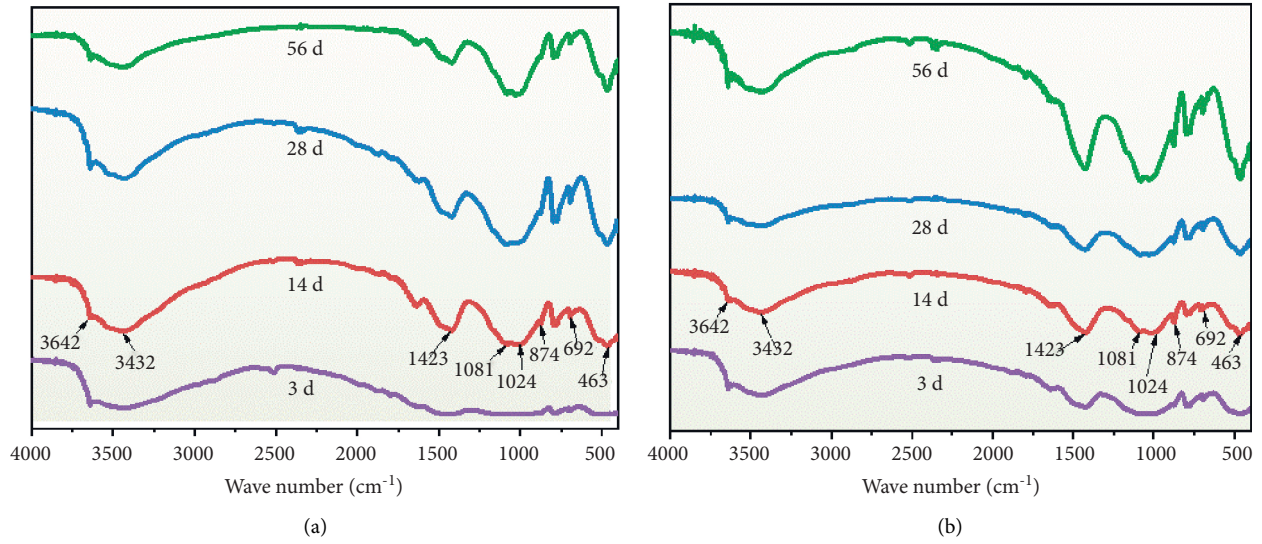
(a)

(b)

FIGURE 10: FTIR spectra of different ages: (a) S-Non; (b) S-100-0.200%.
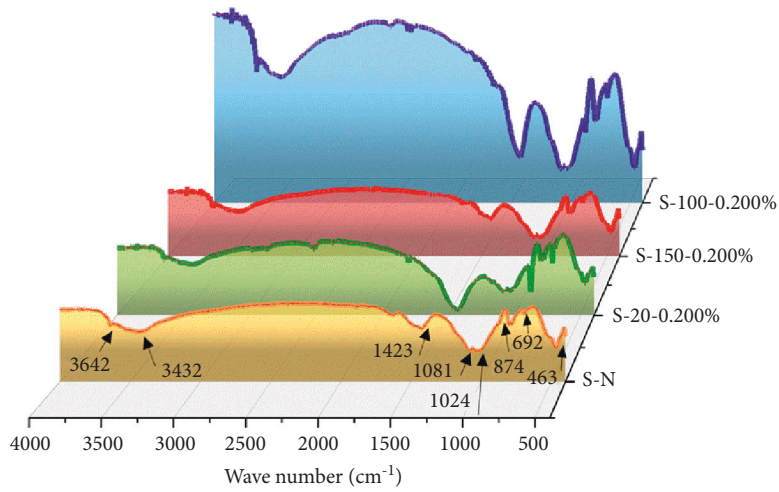

FIGURE 11: FTIR spectra of different particle sizes for 56 d.
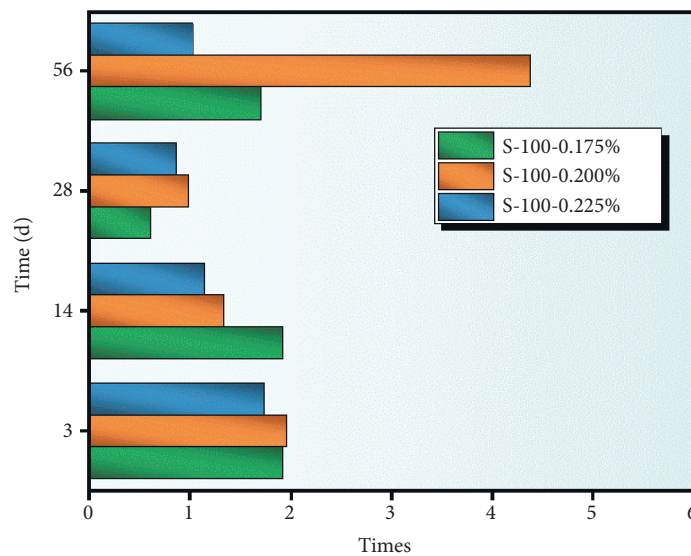

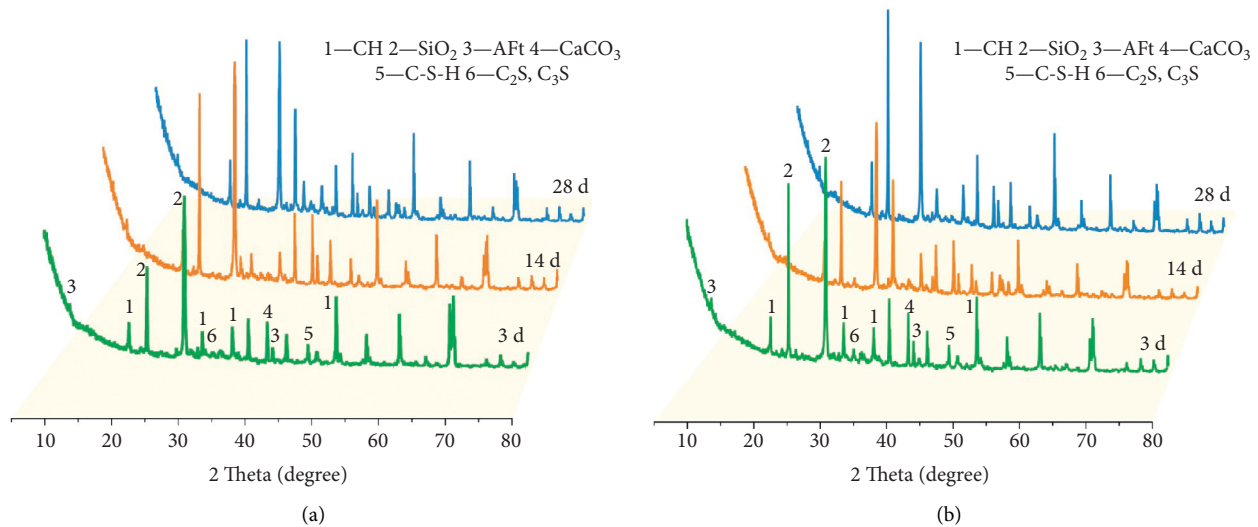FIGURE 12: Ratio of $Ca(OH)_2$ peak area in hydration products at different ages.

FIGURE 13: XRD results at different ages: (a) S-Non; (b) S-100-0.200%.

4.2.2. Analysis of XRD Pattern.

For better understanding of the hydration degree of internal curing concrete, the comparison of the XRD spectrum between S-Non and S-100-0.200% on day 3, day 14, and day 28 is depicted in Figure 13

In Figure 13, it can be clearly obtained that $Ca(OH)_2$, C-S-H gel, and AFt were the main hydration products corresponding to the diffraction peaks of concrete. Besides, SiO_2 from binding material and fine aggregate minerals and the carbonation product of $CaCO_3$ existed. There was no obvious new diffraction peak in the XRD spectrum of S-100-0.200% on day 3, day 14, and day 28, which indicated that the type of hydration product was not changed with the incorporation of SAP.

Compared with the two groups, the content of hydration products was raised with the increase of age. The $Ca(OH)_2$ and AFt diffraction peaks in S-100-0.200% were significantly higher than S-Non. The strongest diffraction peaks of $Ca(OH)_2$ between the group without SAP and internal curing group were 486 Å and 902 Å, and those of C_2S and C_3S were 428 Å and 284 Å, respectively. It could be explained that SAP can promote the consumption of C_2S and C_3S, leading to the generation of more $Ca(OH)_2$.

The above analysis proves once again that the hydration degree of cement concrete is improved through SAP's water release effect; thereby, the microcracks are decreased and the density of the structure is increased, which would prevent the harmful substances such as carbon dioxide from entering the concrete.

4.3. Microstructure and Influence Mechanism of Carbonation.

The factors affecting the carbonation resistance of internal curing concrete mainly include the following two aspects: (1) the compactness of concrete filled by the hydration products generated in the hydration process; (2) the balance between remaining pores formed by SAP gels and hydration product filling effect. Therefore, microstructure analysis of cement concrete and the remaining pores formed by SAP gels should be implemented in the research on carbonation resistance of concrete.

SEM micrographs of S-Non and S-100-0.200% at the magnification of 5000 times at different ages are illustrated in Figures 14 and 15. It can be observed that the number of hydration products of the two groups increased gradually with the increment of age within day 56. The hydration degree of cement concrete structure in the control group is low. Figures 14(a) to 14(d) show that the pores between particles were large with microholes, which led to the distribution of relatively loose microstructure. Compared with the two groups, it can be found that the hydration products in S-Non were less than those in the internal curing group and only a few $Ca(OH)_2$ and a small amount of C-S-H were identified, which was improved at day 56. Obviously, cotton flocculent fibrous C-S-H appeared at day 14 in the S-100-0.200%, and the internal structure became dense. At day 56, a large amount of C-S-H gel was produced, which indicated a higher degree of hydration.

Combined with the micromorphology of internal pores (Figure 16) and the remaining pores formed by SAP gels panorama of S-100-0.200% (Figure 17), the connection between microstructure and performance results of SAP-concrete was clarified, and the influence mechanism of carbonation on internal curing could be mainly interpreted.

As seen in Figure 16, the abundance of hydration products inside the internal pores included the layered $Ca(OH)_2$, flocculent and fibrous C-S-H gel, and a small amount of AFt, which were closely intertwined and overlapped, showing the discontinuous three-dimensional network structure distribution. A large number of C-S-H gel and the accumulation of hydration products on day 56 are presented in Figure 16(b), which indicates the quantity of hydration products was increased and the dense structure was formed; thus, S-100-0.200% showed a better performance than the control group in hydration degree and carbonation test.
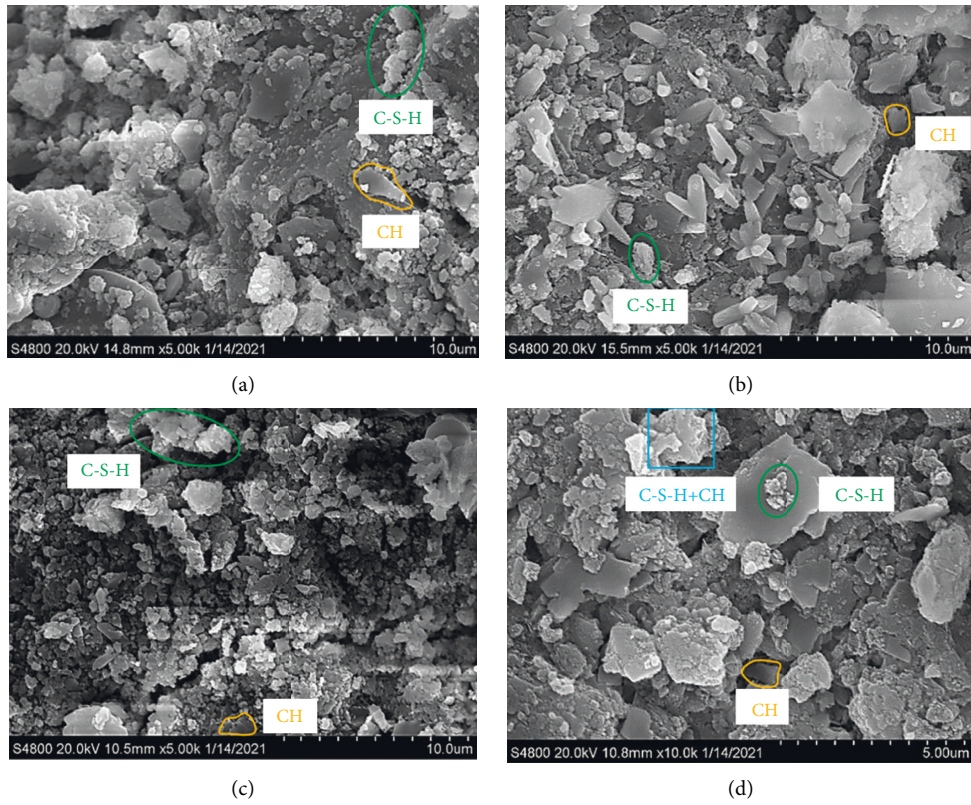
Figure 14: Micromorphology of cement concrete at different ages of control group: (a) 3 d, (b) 14 d, (c) 28 d, and (d) 56 d.
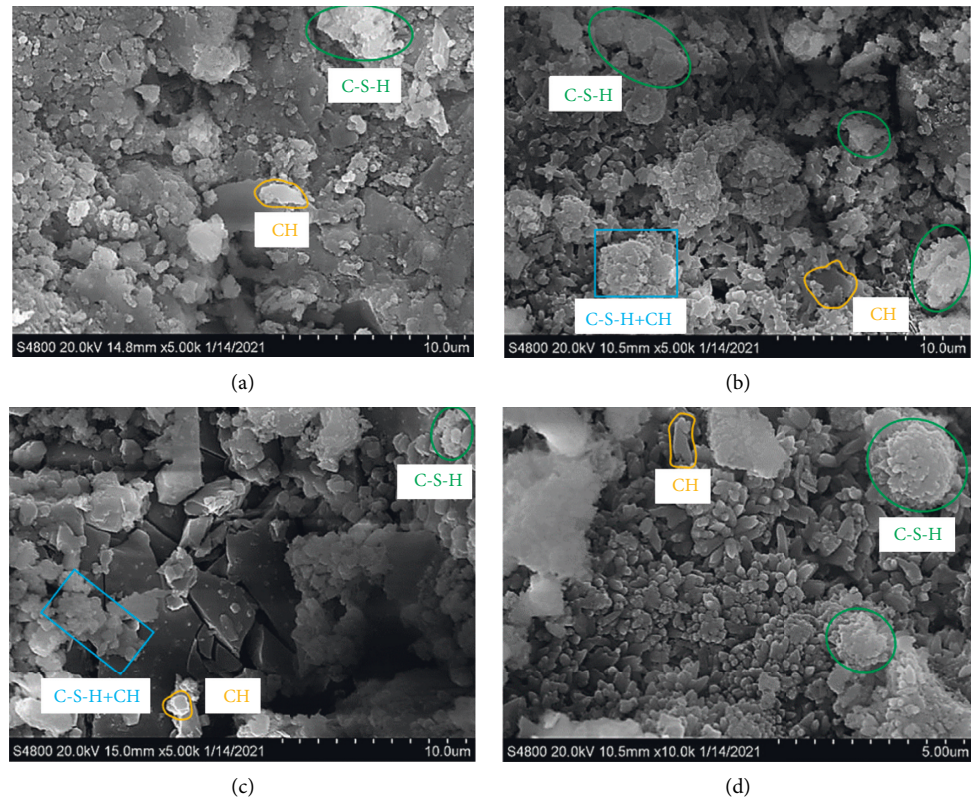

Figure 15: Micromorphology of cement concrete at different ages of S-100-0.200%: (a) 3 d (b) 14 d, (c) 28 d, and (d) 56 d.
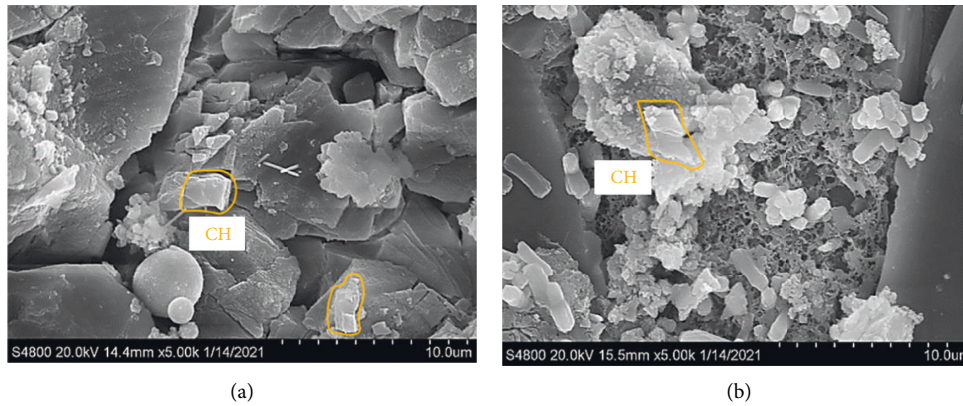
Figure 16: Micromorphology of internal pores of S-100-0.200%: (a) 28 d; (b) 56 d.
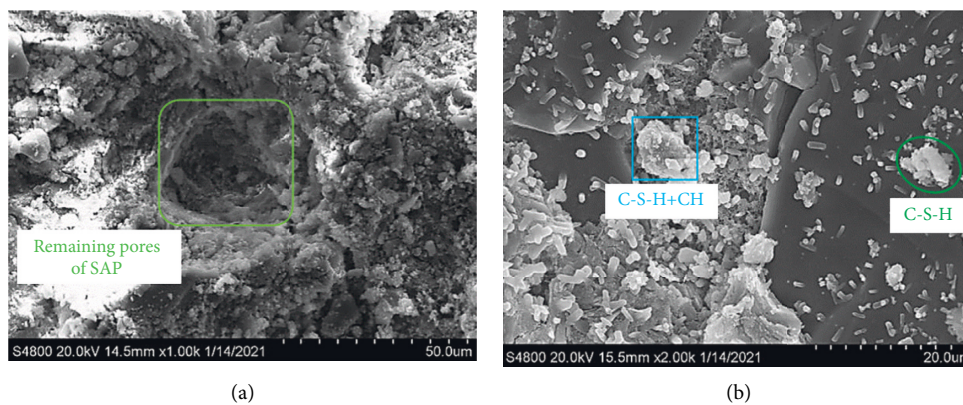

Figure 17: Remaining pores formed by SAP gels panorama of S-100-0.200%: (a) 28 d; (b) 56 d.

As observed in Figure 17(a), the remaining pores formed by SAP gels on day 28 were filled with flocculent SAP and surrounded by a C-S-H gel layer with different thicknesses, which was formed by the diffusion of the slurry around the SAP hole to SAP. It could be analyzed that the large pores would be formed after water release; however, the pore filling of the gel layer is limited and the hydration products are mainly used to fill the opening pores capillary. Failure to achieve effective filling would accelerate the carbonation reaction with the increase of concrete pores, which is a good explanation for the above interesting phenomenon that the particle size of 20 mesh has the worst carbonation resistance among the internal curing group. Moreover, it can be observed from Figure 17(b) that the remaining pores formed by SAP gels could be well filled by hydration products during the internal curing process, which was closely integrated with the boundary; thus, the invasion of CO_2 was blocked.

The improving mechanism of hydration performance and carbonation resistance of SAP-concrete could be concluded based on the above analysis. On the one hand, SAP can compensate for the internal humidity of concrete and make the humidity distribution more uniform during the curing process, which could promote the hydration degree of cement and inhibit the microcracks; otherwise, more hydration products are produced to fill the inside structure. On the other hand, the filling relationship between hydration products and remaining pores formed by SAP gels could be better balanced with the moderate dosage and particle size. Thus, the compactness and integrity of concrete structures are enhanced. The denser the concrete is, the slower the diffusion rate of CO_2 and the smaller the residual pores are. At the same time, the content of alkaline substances is increased; therefore, the more corrosive substances (mainly CO_2 and some H^+, SO_4^{2-}) are needed to consume when entering the internal concrete, which mitigates the diffusion rate of CO_2. Thereby, the carbonation resistance of concrete was reinforced.

5. Conclusions

The carbonation test and hydration degree test included FTIR and XRD of internal curing cement with SAPs of different particle sizes and dosages studied in this article. The micromorphology and remaining pores formed by SAP gels panorama were also investigated to further understand the influence mechanism of internal curing with SAP. The conclusions were summarized as follows:

(1) The carbonation depth of cement concrete at different ages was measured in this research. The carbonation resistance first increased and then decreased with the increase of SAP particle size and

dosage. S-100-0.200% had the best performance, with the carbonation depth of only 56.5% of the control group on day 28. Furthermore, those of S-100-0.175% and S-100-0.225% were 35.8% and 18.2% lower than that of S-Non, respectively. The results showed that the carbonation resistance could be improved effectively by selecting the appropriate SAP particle size and dosage.

(2) The conclusion that the addition of SAP could promote the hydration degree was proved by qualitatively and quantitatively analyzing FTIR spectra and XRD. The area of $Ca(OH)_2$ absorption peak in S-100-0.200% was 3.36 times larger than that of S-Non at day 56. The strongest diffraction peaks of $Ca(OH)_2$ between the control group and S-100-0.200% were 486 Å and 902 Å, and those of C_2S and C_3S were 428 Å and 284 Å, which demonstrated that more C_2S and C_3S translated into $Ca(OH)_2$.

(3) The abundant hydration products in the cement concrete of S-100-0.200% had evenly filled up the remaining pores formed by SAP gels and a dense microstructure was formed, which improved the compactness of concrete and prevented carbon dioxide from entering; thus, the carbonation resistance was enhanced.

(4) The appropriate particle size and dosage obtained by optimization are 100 mesh and 0.200% when W/C is 0.37.

Further work can be performed to simulate the multiple environmental coupled effects like carbonation, salt freeze-thaw cycle, sulfate dry-wet cycle, acid rain, and fatigue load. The resistance performance of SAP-concrete under the multiple environmental coupled effect should be explored and the influencing mechanical properties need to be further clarified.

Data Availability

The data used to support the findings of this study are included within the article.

Conflicts of Interest

The authors declare that there are no conflicts of interest regarding the publication of this article.

Acknowledgments

References

[1] X. Zhang, B. Liu, L. Yang, and Y. Luo, "Experimental study on concrete carbonation performance under the influence of different temperature and strength," *Building Structure*, vol. 50, no. 24, pp. 110–115, 2020.

[2] T. Li, X. Liu, and Y. Zhang, "Carbonization mechanism of reactive powder concrete with sea-water and sea sand," *Materials Reports*, vol. 34, no. 4, pp. 8042–8050, 2020.

[3] F. Tong, Q. Ma, and X. Hu, "Triaxial shear test on hydrochloric acid-contaminated clay treated by lime, crushed concrete, and super absorbent polymer," *Advances in Materials Science and Engineering*, vol. 201913 pages, Article ID 3865157, 2019.

[4] X. Qin, A. Shen, J. Li, and Z. Xie, "Water transport characteristics and mechanical properties of internal curing pavement concrete," *Journal of Building Materials*, vol. 34, no. 3, pp. 606–614, 2021.

[5] D. Shen, C. Liu, J Jiang, J. Kang, and M. Li, "Influence of super absorbent polymers on early-age behavior and tensile creep of internal curing high strength concrete," *Construction and Building Materials*, vol. 258, pp. 120068–120079, 2020.

[6] I. S. Kim, S. Y. Choi, Y. S. Choi, and E. I. Yang, "Effect of internal pores formed by a superabsorbent polymer on durability and drying shrinkage of concrete specimens," *Materials*, vol. 14, no. 18, p. 5199, 2021.

[7] X. Zheng, M. Han, and L Liu, "Effect of superabsorbent polymer on the mechanical performance and microstructure of concrete," *Materials*, vol. 14, no. 12, p. 3232, 2021.

[8] B. J. Olawuyi, A. J. Babafemi, and W. P. Boshoff, "Early-age and long-term strength development of high-performance concrete with SAP," *Construction and Building Materials*, vol. 267, p. 121798, 2021.

[9] D. Dai, J. Peng, X. Zhao, G. Li, and L. Bai, "Strength and road performance of superabsorbent polymer combined with cement for reinforcement of excavated soil," *Advances in Civil Engineering*, vol. 202116 pages, Article ID 9170431, 2021.

[10] X. Qin, J. Xu, A. Shen, and Z. Lyu, "Salt frost resistance and fatigue characteristics of self-curing pavement concrete," *Bulletin of the Chinese Ceramic Society*, vol. 40, no. 8, pp. 2784–2793, 2021.

[11] S. Gupta, "Effect of presoaked superabsorbent polymer on strength and permeability of cement mortar," *Magazine of Concrete Research*, vol. 70, no. 9, pp. 473–486, 2018.

[12] H. Beushausen, M. Gillmer, and M. Alexander, "The influence of superabsorbent polymers on strength and durability properties of blended cement mortars," *Cement and Concrete Composites*, vol. 52, pp. 73–80, 2014.

[13] C. Shi, G. Lyu, X. Ma, J. Zhang, and J. Liu, "Influence of SAP on the properties of self- compacting concrete," *Materials Reports*, vol. 29, no. 20, pp. 118–124, 2015.

[14] L. Zhang, X. Kong, F. Xing, X. Fu, and B. Dong, "Chloride ion invasion and carbonation property of internal cured concrete with super-absorbent polymer," *Journal of Henan University of Science and Technology(Natural Science)*, vol. 40, no. 1, pp. 60–65+7, 2019.

[15] Y. Guo, Z. Huang, W. Wang, A. Shen, and D. Li, "Investigation of carbonation resistance and mechanism of SAP internal curing concrete in humid and hot environment," *Journal of Building Materials*, vol. 25, no. 1, pp. 16–23, 2022.

[16] Y. Jiang, Z. Jin, Y. Chen, and J. Fan, "Effect of super-absorbent polymer on hydration and compressive strength of concrete," *Materials Reports*, vol. 31, no. 24, pp. 40–44+49, 2017.

[17] H. Zhao, Y. Wan, J. Xie, and K. D. X. S. R. G. Jiang, "Effects of nano-SiO2 and SAP on hydration process of early-age cement paste using LF-NMR," *Advances in Materials Science and Engineering*, vol. 2020, Article ID 6089482, 9 pages, 2020.

[18] G. Qin, M. Gao, C. Pang, and W. Sun, "Research on performance ImproVement of ExpansiVe concrete with internal curing agent SAP and its action mechanism," *Journal of Building Materials*, vol. 14, no. 3, pp. 394–399, 2011.

[19] L. P. Esteves, "On the hydration of water-entrained cement-silica systems: combined SEM, XRD and thermal analysis in cement pastes," *Thermochimica Acta*, vol. 518, no. 1-2, pp. 27–35, 2011.

[20] X. Qin, A. Shen, Z. Lyu, and L. J. H. Shi, "Research on water transport behaviors and hydration characteristics of internal curing pavement concrete," *Construction and Building Materials*, vol. 248, pp. 118714–118728, 2020.

[21] GB 175-2020, *Common portland cement*, Standards Press of China, China, 2007.

[22] JGJ 63-2006, *Standard of Water for concrete*, pp. 3-4, ChinaChina Architecture & Building Press, 2006.

[23] JTG3420-2020, *Testing Methods of Cement and Concrete for Highway Engineering*, pp. 237–239, China Communications Press, China, 2020.

[24] R. Hu, W. Liu, L. Xu, L. Jin, and J. G. Liu, "Online analysis method of cement raw materials based on fourier transform infrared spectroscopy," *Spectroscopy and Spectral Analysis*, vol. 40, no. 1, pp. 41–47, 2020.